

Quasiparticle alignment in the most deformed krypton isotope ^{74}Kr

S. L. Tabor, P. D. Cottle, J. W. Holcomb, T. D. Johnson, and P. C. Womble
Physics Department, Florida State University, Tallahassee, Florida 32306

S. G. Buccino and F. E. Durham
Department of Physics, Tulane University, New Orleans, Louisiana 70118
 (Received 29 January 1990)

High-spin states in ^{74}Kr were studied using the $^{58}\text{Ni}(^{19}\text{F},p2n)^{74}\text{Kr}$ reaction at 62 MeV. States up to (14^+) in the ground state band and a number of states in three side bands were placed in the level scheme. The level scheme of ^{74}Kr closely resembles those of ^{76}Kr and ^{78}Kr . Quasiparticle alignment occurs at $\hbar\omega \approx 0.65$ MeV in agreement with a recent calculation. There is no evidence for an alignment at lower frequency as was previously reported. Mean lifetimes were measured for six states in the ground state band of ^{74}Kr using the Doppler shift attenuation and recoil-distance methods. The lifetimes imply transition quadrupole moments of 3.2–3.3 eb, the highest known among Kr isotopes. The corresponding axial deformation is $\beta_2 \approx 0.41$.

I. INTRODUCTION

The Kr isotopes with a half-filled neutron shell ($N \approx 39$) exhibit highly deformed rotational bands coexisting with nearly spherical states of similar energies. Surveys^{1,2} of deformation as a function of occupancy of the f - p - g shell show that maximum deformation is reached at midshell. The even Kr isotopes closest to midshell are ^{74}Kr ($N=38$) and ^{76}Kr ($N=40$). Although these two isotopes would be equally deformed if shell occupancy were the only factor involved, the surveys based on the lowest energy states suggest that ^{76}Kr is somewhat more deformed. However, these are the states most affected by mixing with another coexisting shape, an effect which is known to also vary with neutron number,^{3,4} as discussed in Sec. V. Therefore the energies and lifetimes of higher energy states must be studied to compare the deformations in the yrast rotational bands.

In addition to measuring the lifetimes of higher lying states, another reason for studying ^{74}Kr was to reexamine its energy level scheme. The existing level scheme⁵ does not closely resemble those of the nearby isotopes^{6,7} ^{76}Kr and ^{78}Kr , especially as regards the nonyrast structures. Recent Hartree-Fock-Bogolyubov cranking calculations,⁶ which agree rather well with the measured band crossings in $^{76,78}\text{Kr}$, predict that the proton and neutron alignments should occur at the same frequency in ^{74}Kr , rather than giving rise to two discontinuities in the moment of inertia as had been previously reported.

Roth *et al.*⁵ have previously studied the high-spin states of ^{74}Kr . They have followed the yrast decay sequence through two band crossings up to a spin of $20\hbar$. Three side bands were also reported. They measured the lifetimes of the lowest 2^+ and 4^+ states using the recoil-distance method. The first five transitions in ^{74}Kr had also been observed in an earlier experiment.⁴

The nucleus ^{74}Kr is somewhat difficult to populate because of its distance from the valley of stability. We have used the $^{58}\text{Ni}(^{19}\text{F},p2n)$ reaction at 62 MeV, which is pre-

dicted by statistical model calculations to populate ^{74}Kr as strongly as any other available reaction. The predicted yield of ^{74}Kr is only 4.5% of the total evaporation residues—only about twice the strength of some super deformed bands. γ - γ coincidence relations and directional correlation ratios have been used to construct the level scheme of ^{74}Kr . The mean lifetimes of states in the ground state band were measured using the Doppler shift attenuation and recoil-distance methods.

II. EXPERIMENTAL PROCEDURE

A 62 MeV ^{19}F beam from the Florida State University FN tandem accelerator was used to produce ^{74}Kr via the $^{58}\text{Ni}(^{19}\text{F},p2n)^{74}\text{Kr}$ reaction. A 19 mg/cm² thick rolled Ni foil enriched to 99.9% in ^{58}Ni was used for the target in the γ - γ coincidence experiment. An 0.4 mg/cm² thick natural Ni foil spaced 0.25 or 0.63 mm from a Ta catcher foil was used to measure longer lifetimes using the recoil-distance method.

Two 25% efficient high-purity Ge detectors with axial bismuth germinate Compton suppressors⁸ were placed perpendicular to the beam, while a third was placed at an angle of 4°. A fourth detector of similar efficiency but without a Compton suppressor was located in the backward hemisphere at 140° relative to the beam direction. The target to detector distances were about 10 cm.

Over 6×10^8 γ - γ coincidences were recorded using the 19 mg/cm² thick target. On playback, channel numbers were converted into energies using linear calibrations based on the following lines in the spectra: 74.9 keV (Pb x ray), 188.4 (^{74}Br), 197.15 (^{19}F), 511.0 ($\gamma^+ -$), 634.8 (^{74}Se), and 1000.2 (^{71}As). Average deviations from the linear fits were about 0.1 keV. After calibration the coincident events were histogrammed into four two-dimensional arrays corresponding to the four angle pairs. Where possible, coincidence spectra for a particular angle gated by each of the other detectors were added together.

III. CONSTRUCTION OF THE LEVEL SCHEME

The sum of the 90° spectra in coincidence with the three lowest transitions in the ground state band (GSB) of ^{74}Kr is shown in Fig. 1. The lines in the GSB are clearly visible, as are the narrow, high-energy interband transitions.

The directional correlation of oriented nuclei (DCO) ratios were calculated where possible to determine the multipolarities of the transitions. They are listed in Table I. The DCO ratio R_{DCO} is given by the intensity of a given line in the 4° spectrum gated by a transition in the 90° detectors divided by the intensity of the same line in the 90° spectrum gated by the same gating transition in the 4° detector. The gate transitions were either the 456 or 558 keV lines or the sum of the 456, 558, and 768 keV lines (all with $\Delta J=2$).

The level scheme of ^{74}Kr based on the present work is shown in Fig. 2. Since there are differences from the previously published level scheme,⁵ a detailed discussion of the present assignments follows.

A. Ground state band

The 456.1, 558.2, 768.3, 966.9, and 1144.6 keV peaks in Fig. 1 agree within 1 keV with the first five GSB transitions previously reported⁵ in ^{74}Kr . Their coincidence relations, intensities, and Doppler shift attenuations confirm that placement. However, only a very weak peak is seen near 1125 keV, which was previously assigned as the transition above 1145 keV. The spectrum gated on

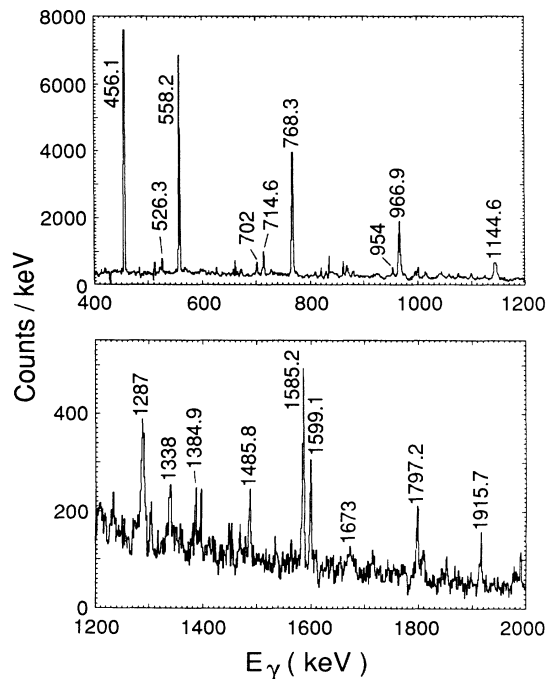


FIG. 1. The spectrum of γ rays at 90° in coincidence with the 456.1, 558.2, and 768.3 keV transitions in ^{74}Kr .

TABLE I. Directional correlation of oriented nuclei (DCO) ratios based on the 4° and 90° intensities of transitions in ^{74}Kr .

E_γ (keV)	E_I (keV)	E_F (keV)	R_{DCO}
456.1	456.1	0	1.09(5)
483.5	3139.8	2656.5	1.50(40)
526.4	3139.8	2613.4	0.58(15)
558.2	1014.3	456.1	0.99(5)
702	3842	3139.8	1.29(21)
714.6	2656.5	1941.9	1.30(30)
768.3	1782.6	1014.3	0.97(7)
954	5088	4134	0.84(20)
966.9	2749.5	1782.6	0.96(8)
1144.6	3894.1	2749.5	0.93(10)
1287	5181	3894.1	1.05(15)
1338	6519	5181	0.87(20)
1384.9	4134	2749.5	0.59(23)
1485.8	1941.4	456.1	1.11(12)
1585.2	3367.5	1782.6	0.54(11)
1599.1	2613.4	1014.3	0.69(15)
1797.3	2811.5	1014.3	0.52(15)

the 1125 keV region shows very little evidence for other ^{74}Kr lines. On the other hand, the 1287 keV peak, which is in coincidence with lower GSB transitions, has the right intensity and Doppler-broadened width to be the sixth GSB transition ($12^+ \rightarrow 10^+$). This appears to correspond to the previously reported 1290 keV line, which had been assigned as the (14^+) \rightarrow (12^+) transition. We also see no evidence for an 888 keV line which was proposed as the other decay path of the 12^+ state.

The 1338 keV peak in Fig. 1 appears to be the seventh GSB transition. The spectrum gated by it clearly shows lower members of the GSB, but the statistics are too limited to determine whether the 1145 and 1287 keV lines are in coincidence with it. The 1338 keV line probably corresponds to the previous 1335 keV transition which was assigned as the (16^+) \rightarrow (14^+) decay.

We see no evidence for a 1616 keV line which was previously assigned as the (18^+) \rightarrow (16^+) transition. A broad peak at 1673 keV is a good candidate for the eighth GSB transition. It has not been shown on the level scheme because the statistics are too weak to conclude whether it is in coincidence with transitions above the 8^+ state or whether there are any intervening transitions.

Roth *et al.*⁵ assigned a 1995 keV transition to the (20^+) \rightarrow (18^+) decay. Our spectrum shows a 1990 keV line which is far too narrow to feed higher members of the GSB and a broad 1983 keV peak whose width is appropriate. Even if the 1983 keV peak represents the GSB transition corresponding to the previous 1995 keV assignment, one must examine the broad peak at 1802 keV (under the 1797 keV line) which may be another GSB transition.

The DCO ratios for the first six GSB transitions are close to unity, consistent with quadrupole transitions and in support of the spin assignments shown in Fig. 2. That for the 1338 keV transition is consistent with unity and $\Delta J=2$, but its somewhat lower value and larger uncertainty cannot rule out $\Delta J=1$ conclusively.

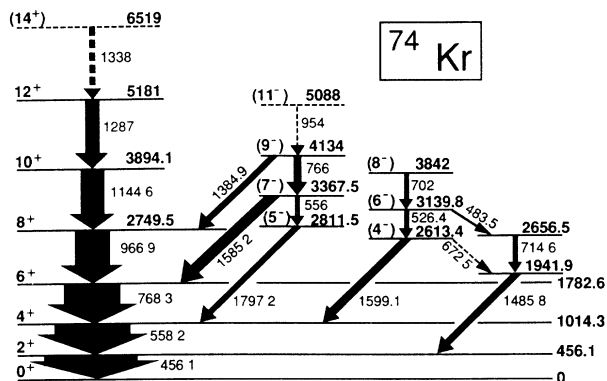


FIG. 2. The energy level scheme of ^{74}Kr deduced from the present work.

B. Side bands

A number of high-energy, relatively narrow lines can be seen in Fig. 1. Most of these have DCO ratios of about one-half, characteristic of dipole transitions. They represent decays connecting the side bands with the GSB.

The 1585 keV transition appears to correspond to the previously assigned 1584 keV decay.⁵ The 768 keV line in the 1585 keV gate clearly shows a low energy tail which gives a centroid of 765–766 keV when the entire line shape is fitted to the sum of two Gaussian curves. This corresponds to the previous 765 keV transition. Its location close to the stronger 768 keV line is inconvenient for determination of an accurate energy and detailed coincidence relations.

The 1385 keV line feeds the 8^+ GSB state and energy sums suggest that it depopulates the same 4134 keV state as does the 766 keV decay. This line has not been discussed previously, and we see no evidence for an 888 keV transition above the 766 keV one. There is a weak 954 keV peak in coincidence with the 1585 keV and lower GSB transitions. However, it is too weak to determine if it is in coincidence with the 766 and 1385 keV lines.

The 1797 keV transition feeds into the 4^+ GSB state. This implies a level at 2811.5 keV—556 keV below the 3367.5 keV parent state of the 1585 keV decay. The 1797 keV gate reveals another inconvenient doublet with a 555–556 keV tail on the strong 558 keV peak.

The DCO ratios of the 1385, 1585, and 1797 keV lines are close to one-half, implying dipole transitions. This rules out the previous 8^+ assignment to the 3367.5 keV level. The DCO ratio of the 954 keV line is somewhat indeterminate, although closer to unity. It was not possible to determine DCO ratios for the poorly resolved 556 and 766 keV peaks. Spin sequences of 5, 7, 9, and 11 or 4, 6, 8, and 10 are consistent with the DCO ratios. The close similarity in energy spacing and decay pattern to the negative parity, odd spin rotational band^{6,7} in ^{76}Kr suggests a spin-parity sequence of $5^-, 7^-, 9^-,$ and 11^- .

The 1599 keV transition also feeds into the yrast 4^+ state and is in coincidence with additional lines at 526 and 702 keV. Although the 526 and 702 keV lines clearly satisfy the coincidence relations implied by their placement in the level scheme, they are also strongly in coin-

cidence with known ^{74}Se and ^{71}As lines, respectively.

The DCO ratio of the 1599 keV transition is consistent with dipole decay. The aforementioned doublet nature of the 526 and 702 keV lines suggests that their DCO ratios should be interpreted with caution. The somewhat lower transition energies in this band compared with those in the band discussed earlier and the comparison with the negative parity, even spin band in ^{76}Kr suggest the spin sequence $4^-, 6^-,$ and 8^- for the present band. A further correspondence with the ^{76}Kr band is the decay branch to a fourth band.

The 1486 keV transition, which is in coincidence with only the 456 keV GSB transition, is also in coincidence with 484, 702, and 715 keV lines. This implies two members of a fourth decay sequence which is also fed from the third band discussed above. There is also some evidence for a 672.5 keV interband transition, but it is too weak to establish all the coincidence relations. The 715 keV transition has been placed here knowing that the $13/2^+ \rightarrow 9/2^+$ transition in ^{71}As has a similar energy. There is no evidence for a 392 keV transition in coincidence with the 1486 keV line as was previously proposed,⁵ nor for 558–1486 keV coincidences.

The evidence for spins in this band is less clear. The DCO ratio for the 715 keV line is consistent with quadrupole decay, but it may be contaminated by the ^{71}As line. That for the 1486 keV peak is also about unity and consistent with quadrupole decay. This evidence implies a spin sequence of $4^+, 6^+$. On the other hand, the 6^- state in ^{76}Kr decays to the 5^+ , not 6^+ , state, and many other close similarities with ^{76}Kr have been seen. It is also the 3^+ state in ^{76}Kr which decays to the lowest 2^+ level. Hence the analogy with ^{76}Kr suggests spins of 3^+ and 5^+ for the two states in this band. There are values of the $E2/M1$ mixing ratio which would give the measured DCO ratio for the 1486 keV transition if $J^\pi = 3^+$ for the 1942 keV state, but the spin question remains somewhat open at present.

C. Other transitions

There are still some high-energy transitions not placed in the level scheme. Most notable is the 1916 keV line which feeds into the 6^+ or 8^+ level. The strong ^{74}Se lines in the 1916 keV gate and the similarity in energy of the 967 keV lines in ^{74}Se and ^{74}Kr make it difficult to establish whether the 1916 keV peak is in coincidence with the $8^+ \rightarrow 6^+$ transition in ^{74}Kr . The 1395 keV peak in Fig. 1 appears to be in coincidence only with a 455.5 keV transition in ^{71}As and may not represent a ^{74}Kr transition.

We see no evidence for a 723 keV transition feeding the 2^+ state, nor for any of the transitions proposed above it.⁵ The 968 keV peak in Fig. 1 is not inconsistent with a weak 963 keV shoulder, but no clear coincidence relations can be established with the possible 963 keV line. There is evidence for a 1015 keV peak in Fig. 1, but it is not stronger than some known contaminant peaks. The 1015 keV gate shows very weak peaks at 456, 558, and possibly 768 keV, but none at 299, 375, 499, 570, 723, 798, or 963 keV, which were previously reported in the level scheme.

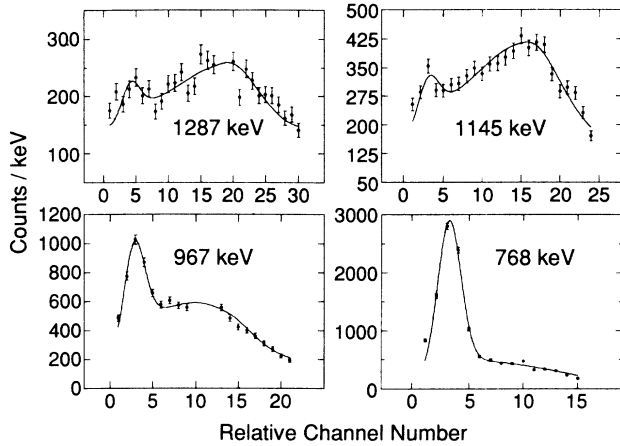


FIG. 3. Doppler-shifted line shapes observed at 4° in coincidence with the first two or three transitions in ^{74}Kr . The smooth lines represent fits with a simulation program.

IV. MEAN LIFETIMES

A. Doppler shift attenuation method

The mean lifetimes of states in the GSB were measured using the Doppler shift attenuation method (DSAM). Line shapes in the spectrum of the 4° detector gated by transitions seen in any of the other detectors were fitted by a simulation program. The gating transitions were the first three in the GSB except for the 768 keV line shape for which only the first two were used. The initial ^{74}Kr recoil velocity was about 2% of the speed of light.

The program⁹ simulated by numerical integration the decay of ^{74}Kr nuclei as they slowed down in the ^{58}Ni target. The tabulated electronic differential energy loss values of Northcliff and Schilling¹⁰ were scaled by a few percent to the experimental α stopping powers¹¹ in Ni at the same velocity. The nuclear component of the stopping powers was calculated using the Bohr ansatz,^{12,13} and the angular straggling due to atomic collisions was treated in Blaugrund's approximation.¹⁴ The program also simulated the projectile deceleration before interaction in the target and used ^{74}Kr production cross sections as a function of beam energy obtained from the statistical

model code PACE2.¹⁵ A Gaussian distribution of recoil speeds following evaporation was used. No variation of recoil angle was used because a simulated distribution of recoil angles was found to have no effect on the 4° spectrum. The finite energy resolution and angle range subtended by the detector were included in the simulation.

The decay simulation included the delays caused by all known feedings above the state of interest as well as by side feeding. A side feeding time of 0.05 ps was used in fitting the 1338 keV line shape. This was increased by about 0.03 ps per state as the cascade proceeded. Much longer side feeding times would not be consistent with the fast transitions seen.

The measured and simulated line shapes for most of the transitions fitted are shown in Fig. 3. The results are summarized in Table II along with the present and previous recoil-distance measurements. The value for the 14^+ state is listed as an upper limit since the direct feeding time into it is not known. None of the transitions observed in or from the sidebands shows any measurable Doppler shifting. This implies lifetimes greater than about 1 ps. The transition quadrupole moments Q_i are calculated from the $E2$ strengths using the simple rotation model. The quadrupole deformations β_2 of an axially symmetric rotor which would give these quadrupole moments are included for comparison.

B. Recoil-distance method

The short experiment (7×10^7 events) with a thin target and a drift distance of 0.25 mm to the catcher foil provided useful information about longer lifetimes in ^{74}Kr . The Doppler shifts at both 4° and 140° gave a consistent drift velocity of $0.0172c$ or a drift time of 49 ps.

No unshifted stopped peak was seen for the 558 keV transition or for any higher ones in the GSB. An upper limit of 7% can be set for any possible 558 keV stopped peak. This provides an upper limit of 18 ps for the lifetime of the 4^+ state, taking into account feeding delays from the 6^+ state ($\tau=0.9$ ps), and is consistent with the previously reported value⁵ of 13.2 ps.

A small, but clear, stopped peak was seen at both 4° and 140° for the 456 keV transition, as shown in Fig. 4. This peak represents 23.2% of the total decay strength and implies a mean life of 23.5 ps for the 2^+ state, after

TABLE II. Mean lifetimes and transition strengths in the ground state band of ^{74}Kr .

J^π	τ (ps)	$\tau(\text{ps})^a$	$B(E2)$ (W.u.) ^b	$ Q_i $ (eb)	β_2^c
2^+	23.5(20) ^d	28.8(57)	95	3.0(1)	0.38
4^+	< 18	13.2(7) ^d	63	2.0(1)	0.26
6^+	0.90(15)		185	3.3(3)	0.41
8^+	0.28(5)		188	3.3(3)	0.41
10^+	0.10(3)		225	3.5(6)	0.44
12^+	0.18(5)		70	1.9(3)	0.26
(14^+)	< 0.20		> 53	> 1.7	> 0.22

^aReference 5.

^b1 W.u. = $18.5 e^2\text{fm}^4$.

^cAssuming axial symmetry.

^dUsed in calculating the transition strength and deformation for this state.

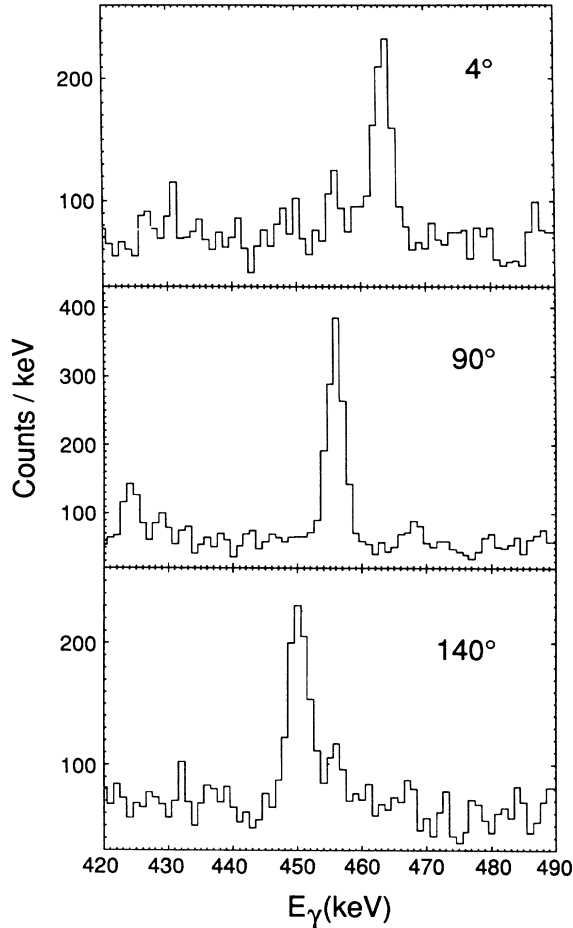


FIG. 4. Spectra observed at three different angles in coincidence with the 558.2 and 768.3 keV transitions in the recoil-distance experiment.

correcting for feeding delays from the 6^+ (0.9 ps) and 4^+ (13 ps) states. This is about one standard deviation below the previous value of 28.8 ± 5.7 ps. It is not entirely derived from the present work because it depends somewhat on the previously reported lifetime of the 4^+ state through the feeding correction.

V. DISCUSSION

A. Systematic comparisons

The level scheme of ^{74}Kr shows close similarities with those^{6,7} of ^{76}Kr and ^{78}Kr . However, it has not been possible to trace the rotational bands as high in spin because ^{74}Kr is populated rather weakly in this and other possible reactions. The transition energies in the GSB of ^{74}Kr are similar, but generally slightly lower, than those in $^{76,78}\text{Kr}$. Three of the four side bands reported in the heavier isotopes have also been seen. Their transition energies are also rather similar, if the tentative identifications of the bands are correct. There is even a close correspondence in the pattern of interband transitions, even down to the $6^- \rightarrow 5^+$ $E1$ decay if the rightmost band in Fig. 2 has odd spin.

These similarities with the heavier isotopes naturally

lead to the question of comparison with the lighter ones. Only very limited information is known³ about the $N=Z$ isotope ^{72}Kr . If the 612.5 and 790.2 keV gamma rays represent the $4^+ \rightarrow 2^+$ and $6^+ \rightarrow 4^+$ transitions, respectively, they are similar to those in ^{76}Kr and slightly higher than those in ^{74}Kr . This would indicate that the deformation in the GSB reaches a maximum in ^{74}Kr and begins to fall as the neutron number drops below mid-shell, as in many other $f-p-g$ shell nuclei.¹ Another interesting trend is in the $2^+ \rightarrow 0^+$ transition energies, which increase somewhat from ^{76}Kr to ^{74}Kr . The increase is so much larger in ^{72}Kr that the $2^+ \rightarrow 0^+$ transition energy (709.1 keV) exceeds that of the $4^+ \rightarrow 2^+$ (612.5 keV). This anomaly was interpreted as a sign of shape coexistence, in analogy with ^{72}Se . Although the effect is more subtle in ^{74}Kr , the cranking analysis (see Sec. V B) shows some distortion of the lowest energy levels, which may be due to mixing with other less deformed states.

There are also similarities between the level schemes of the isotones ^{74}Kr and ^{74}Se , just as was seen between ^{72}Kr and ^{72}Se , although the comparison is complicated by the two mixed coexisting bands in ^{74}Se (Refs. 16–18). The transition energies are higher in ^{74}Se except above the 8^+ state in the yrast band.

B. Cranking model analysis

Of particular interest is the question of quasiparticle alignments in ^{74}Kr , and how they compare with those in neighboring nuclei. Alignments are best observed by analyzing the data in a cranking model framework.¹⁹ The kinematic ($J^{(1)}$) and dynamic ($J^{(2)}$) moments of inertia for the GSB of ^{74}Kr are shown in Fig. 5 along with those^{6,7} of ^{76}Kr and ^{78}Kr .

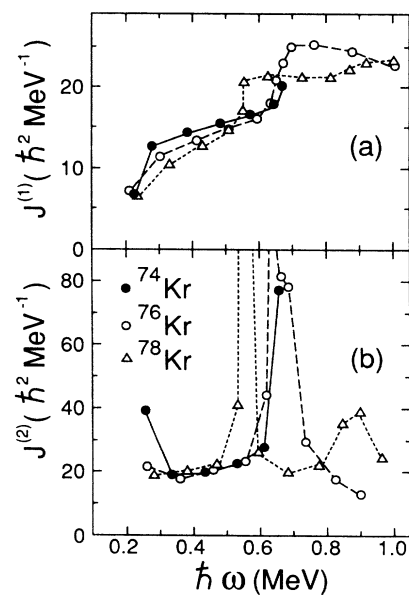


FIG. 5. A comparison of the kinematic ($J^{(1)}$) and dynamic ($J^{(2)}$) moments of inertia for the GSB in three even Kr isotopes. The symbols have the same meaning in both parts of the figure.

Except for the first point, the kinematic moments of inertia of ^{74}Kr are somewhat larger than those of the heavier isotopes [Fig. 5(a)]. This indication that ^{74}Kr is more deformed is confirmed by the transition quadrupole moments to be discussed below.

The upturn above $\hbar\omega=0.65$ MeV is evidence for the onset of quasiparticle alignment. This is better seen in the lower graph of dynamic moments of inertia, which are basically the derivatives of the upper curves. Alignments in the even Kr isotopes can also be compared in the graphs of aligned angular momentum shown in Fig. 6(a). The aligned angular momentum is obtained by subtracting a reference angular momentum which represents the contribution due to collective rotation. For the sake of comparison we have used the same reference ($I_{\text{Ref}}=21\omega-3\hbar$) employed in Ref. 6 for all three isotopes, despite indications that ^{74}Kr is more deformed. This reference was derived from the negative parity bands in the heavier isotopes and is similar to that used in Ref. 7.

Figures 5 and 6 clearly show that quasiparticle alignment in ^{74}Kr begins at $\hbar\omega\approx 0.65$ MeV, as in ^{76}Kr , well after the first alignment in ^{78}Kr . This differs from the pattern implied by the previous ^{74}Kr level scheme⁵ where a large negative excursion occurs in the dynamic moment of inertia at $\hbar\omega\approx 0.57$ MeV before the positive peak near $\hbar\omega=0.65$ MeV. In fact the observed alignment frequency in ^{74}Kr is in excellent agreement with the Hartree-Fock-Bogolyubov cranking calculations of Ref. 6 and Sec. V D. These calculations predict essentially identical proton and neutron crossing frequencies of 0.6 MeV/ \hbar at the predicted prolate deformation of $\beta_2\approx 0.37$. The predicted crossing frequency rises even closer to the observed value of about 0.65 MeV/ \hbar at the slightly higher deformation of $\beta_2\approx 0.41$ implied by the transition

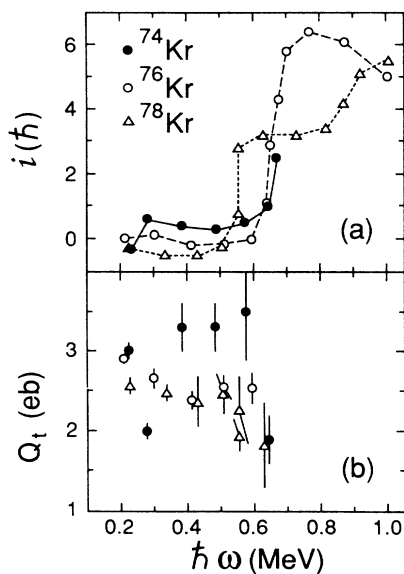


FIG. 6. A comparison of the aligned angular momentum (i) and transition quadrupole moments (Q_t) for the GSB in three even Kr isotopes. The reference angular momentum subtracted to determine i is $I_{\text{Ref}}=21\omega-3\hbar$.

strengths discussed below. It is, of course, unfortunate that the level scheme cannot be established with confidence above the crossing.

The anomalous lowest frequency point for ^{74}Kr in Figs. 5(a), 5(b), and 6(a) deserves further comment. It arises because the $2^+ \rightarrow 0^+$ transition energy is higher than its counterpart in ^{76}Kr even though the higher ^{74}Kr GSB transition energies are lower than those in ^{76}Kr . This appears to be more than an isolated anomaly since the $2^+ \rightarrow 0^+$ transition energy in ^{72}Kr is so large that it exceeds that of the $4^+ \rightarrow 2^+$ transition.³ The effect has been interpreted as evidence for shape coexistence in ^{72}Kr , and it is likely that the same explanation applies to ^{74}Kr . Piercey *et al.*⁴ have also presented evidence for distortion of the low-lying level schemes of $^{74,76,78}\text{Kr}$ as due to mixing between deformed and near spherical bands. The distortion increases with decreasing mass.

C. Transition strengths and deformation

The transition quadrupole moments $|Q_t|$ in Table II, which were determined from the measured lifetimes, are graphed in Fig. 6(b) as a function of rotational frequency. For comparison the $|Q_t|$ values determined from published lifetimes^{6,20,21} in the GSB of ^{76}Kr and ^{78}Kr are also shown in Fig. 6(b). The $|Q_t|$ values are graphed at the rotational frequency intermediate between those of the parent and daughter states, as is done for the kinematic moment of inertia and aligned angular momentum.

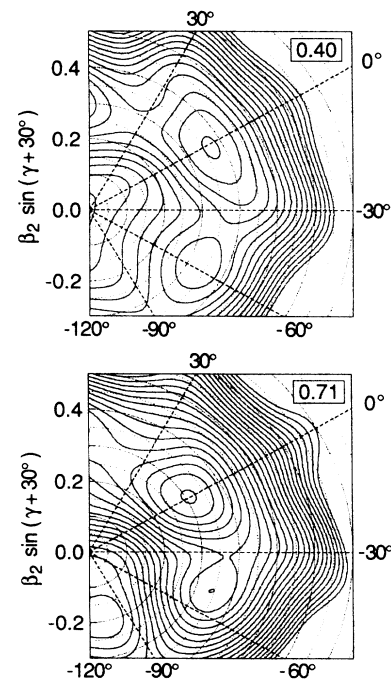


FIG. 7. Total Routhian surfaces (with pairing) in the (β_2, γ) polar coordinate plane for the yrast configuration in ^{74}Kr . The numbers in boxes give the values of rotational frequency in MeV/ \hbar . The distance between contour lines is 500 keV. Dashed lines at some γ angles are labeled in degrees outside the graphs.

With the exception of two points, the transition quadrupole moments in ^{74}Kr lie at or above 3 eb with an average of 3.2–3.3 eb. This is higher than the average values of about 2.5 eb for $^{76,78}\text{Kr}$. The Q_t value at the highest ^{74}Kr frequency that could be measured is significantly lower than the others. This is based on a lifetime measured with corrections for feeding delays above it and may be lower because of the band crossing occurring at this frequency as well as the reduced deformation expected after alignment (see Sec. V D). The low value of Q_t at $\hbar\omega=0.28$ MeV is based on the only lifetime not measured or remeasured in the present work. However, the present value of the lifetime of the 2^+ state is only 20% below the previous value, and such a change in the lifetime of the 4^+ state would not raise Q_t very much. Perhaps this low value is related to weak transitions between coexisting shapes.

The transition quadrupole moments imply an average axial deformation of $\beta_2 \approx 0.41$ for ^{74}Kr . A somewhat smaller deformation would give the observed Q_t values if the shape were triaxial. The Hartree-Fock-Bogolyubov cranking calculations of Ref. 6 and Sec. V D predict an axial prolate deformation of $\beta_2 \approx -0.37$, just a little below the observed value. An earlier calculation²² predicts $\beta_2=0.35$ and $Q_2=3.01$ eb. The deformation observed in ^{74}Kr is similar to the shape of $\beta_2=0.40$, $\gamma=-8^\circ$ inferred from a recent experimental and theoretical study²³ of ^{75}Kr , although the more definitive lifetime measurements are not yet available.

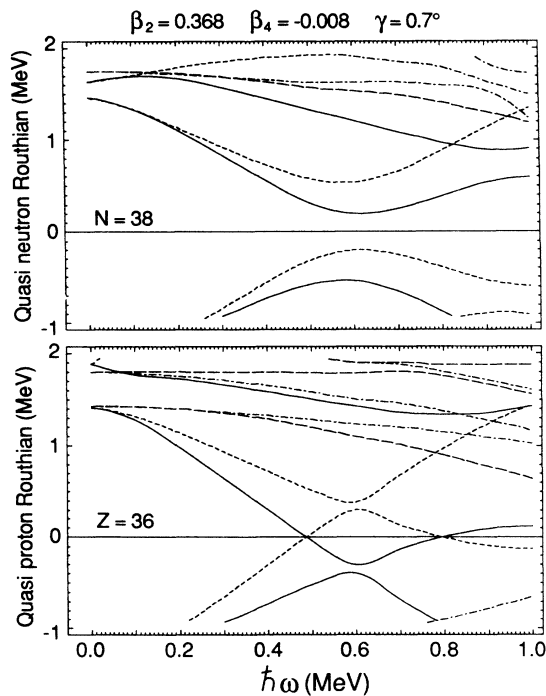


FIG. 8. Quasiparticle Routhians for ^{74}Kr at a deformation of $\beta_2=0.37$, $\gamma=0.7^\circ$, $\beta_4=-0.008$. The spin and parity of the Routhians are indicated in the following way: $(+, \frac{1}{2})$, solid line; $(+, -\frac{1}{2})$, dotted line; $(-, \frac{1}{2})$, dot-dashed line; and $(-, -\frac{1}{2})$, dashed line.

D. Hartree-Fock-Bogolyubov cranking calculations

A theoretical analysis of the high-spin properties of ^{74}Kr has been carried out²⁴ using the Woods-Saxon model of Ref. 22. The pairing force was assumed to be of the monopole type, and the rotation was treated by means of the cranking approximation. The procedure used here has been described in Refs. 9 and 25. The calculations are similar to those reported in Ref. 6, which were discussed above.

The calculated total Routhian surfaces (TRS) in the (β_2, γ) plane for the yrast configuration are shown in Fig. 7 for two rotational frequencies. At each (β_2, γ) grid point the total Routhian was minimized with respect to the hexadecapole deformation β_4 . The TRS shown for $\omega=0.40$ MeV/ \hbar are typical of those below the band crossing. There is a well-defined minimum on the prolate axis ($\gamma=0^\circ$) at $\beta_2 \approx 0.37$ which barely changes with frequency. The secondary minimum on the oblate axis ($\gamma=-60^\circ$) increases in energy relative to the absolute minimum and increases somewhat in deformation with increasing rotational frequency.

The TRS at $\omega=0.71$ MeV/ \hbar is typical of those after the band crossing. The absolute minimum energy point remains prolate ($\gamma=1.5^\circ$) but drops somewhat in deformation ($\beta_2=0.31$). The secondary minimum continues to climb in energy and becomes somewhat triaxial ($\gamma \approx -45^\circ$).

A quasiparticle diagram representative of the calculated zero-quasiparticle configuration ($\beta_2=0.37$, $\gamma=0.7^\circ$) is shown in Fig. 8. It shows that both proton and neutron alignments are predicted to occur at $\hbar\omega \approx 0.60$ MeV.

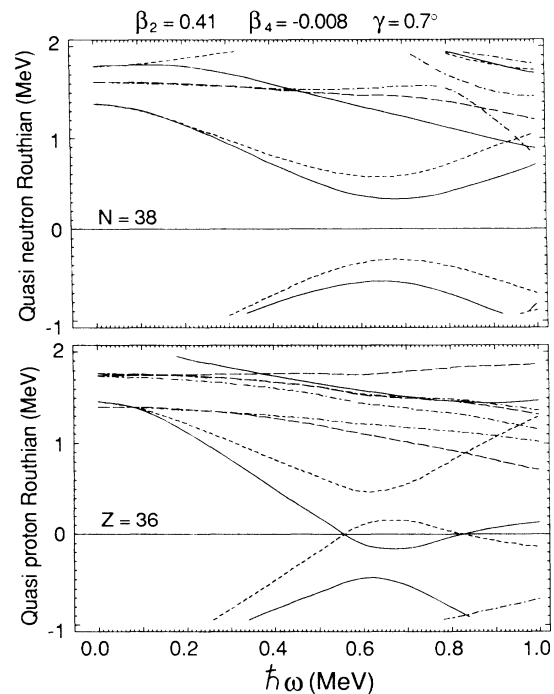


FIG. 9. Quasiparticle Routhians for ^{74}Kr at a deformation of $\beta_2=0.41$, $\gamma=0.7^\circ$, $\beta_4=-0.008$.

Since the measured deformation in ^{74}Kr is a little larger, another quasiparticle diagram is shown in Fig. 9 for $\beta_2=0.41$ and $\gamma=0.7^\circ$. Both proton and neutron alignment frequencies increase somewhat, as was shown graphically in Ref. 6.

VI. CONCLUSIONS

The high-spin structure of ^{74}Kr has been studied up to the (14^+) state in the ground state band and to lower spins in three nonyrast bands. The present level scheme of ^{74}Kr very closely resembles those of its isotopic neighbors ^{76}Kr and ^{78}Kr , emphasizing the value of systematic studies of the Kr nuclei. Even the pattern of interband transitions is quite similar.

A cranking model analysis of the yrast band of ^{74}Kr shows that quasiparticle alignment begins at a rotational frequency of $0.65 \text{ MeV}/\hbar$, in contrast to an earlier study. This frequency agrees well with the predictions of recent Hartree-Fock-Bogolyubov cranking calculations, which also describe the alignments in heavier Kr isotopes well. A recent study of ^{72}Kr gives further weight to a previous interpretation of the pronounced anomaly in the mo-

ments of inertia in ^{74}Kr at low frequency as due to shape coexistence.

Above the low-lying region influenced by shape coexistence, the moments of inertia and transition quadrupole moments show that the ground state band of ^{74}Kr is more deformed than that of ^{76}Kr . This reverses the picture based on the lowest states, but still implies a lack of symmetry about $N=39$ in the deformations. Although only limited information is available on ^{72}Kr , its deformation appears similar to that of ^{76}Kr .

This makes ^{74}Kr the most deformed even Kr isotope. Its transition quadrupole moments average about 3.2–3.3 eb implying an axial deformation of $\beta_2 \approx 0.41$. Theoretical calculations predict a deformation almost as high for ^{75}Kr ($N=39$), but its transition strengths are not yet known.

ACKNOWLEDGMENTS

We are grateful to W. Nazarewicz for providing theoretical calculations on ^{74}Kr . We would like to acknowledge informative discussions with K. P. Lieb and the assistance of J. Baker in data acquisition and analysis.

-
- ¹S. L. Tabor, Phys. Rev. C **34**, 311 (1986).
²S. Raman, C. H. Malarkey, W. T. Milner, C. W. Nester, Jr., and P. H. Stelson, At. Data Nucl. Data Tables **36**, 1 (1987); S. Raman, C. W. Nester, Jr., and K. H. Bhatt, Phys. Rev. C **37**, 805 (1988).
³B. J. Varley, M. Campbell, A. A. Chisti, W. Gelletly, L. Goettig, C. J. Lister, A. N. James, and O. Skeppstedt, Phys. Lett. B **194**, 463 (1987).
⁴R. B. Piercey, J. H. Hamilton, R. Soundranoyagam, A. V. Ramayya, C. F. Maguire, X. -J. Sun, Z. Z. Zhao, R. L. Robinson, H. J. Kim, S. Frauendorf, J. Döring, L. Funke, G. Winter, J. Roth, L. Cleemann, J. Eberth, W. Neumann, J. C. Wells, J. Lin, A. C. Rester, and H. K. Carter, Phys. Rev. Lett. **47**, 1514 (1981).
⁵J. Roth, L. Cleemann, J. Eberth, T. Heck, W. Neumann, M. Nolte, R. B. Piercey, A. V. Ramayya, and J. H. Hamilton, J. Phys. G **10**, L25 (1984).
⁶C. J. Gross, J. Heese, K. P. Lieb, S. Ulbig, W. Nazarewicz, C. J. Lister, B. J. Varley, J. Billowes, A. A. Chishti, J. H. McNeil, and W. Gelletly, Nucl. Phys. A **501**, 367 (1989).
⁷M. S. Kaplan, J. X. Saladin, L. Faro, D. F. Winchell, H. Takai, and C. N. Knott, Phys. Lett. B **215**, 251 (1988).
⁸S. L. Tabor, Nucl. Instrum. Methods **B24/25**, 1031 (1987).
⁹E. F. Moore, P. D. Cottle, C. J. Gross, D. M. Headly, U. J. Hüttmeier, S. L. Tabor, and W. Nazarewicz, Phys. Rev. C **38**, 696 (1988).
¹⁰L. C. Northcliffe and R. F. Schilling, Nucl. Data Sec. A **7**, 233 (1970).
¹¹J. F. Ziegler and W. K. Chu, At. Data Nucl. Data Tables **13**, 463 (1974).
¹²S. Kalbitzer, H. Oetzmann, N. Grahmann, and A. Feverstein, Z. Phys. A **278**, 223 (1976).
¹³J. Lindhard, M. Scharff, and H. E. Schiott, K. Dan. Vidensk. Selsk., Mat.-Fys. Medd. **33**, No. 14 (1963).
¹⁴A. E. Blaugrund, Nucl. Phys. **88**, 501 (1966).
¹⁵A. Gavron, Phys. Rev. C **21**, 230 (1980).
¹⁶R. B. Piercey, A. V. Ramayya, R. M. Ronningen, J. H. Hamilton, V. Maruhn-Rezwani, R. L. Robinson, and H. J. Kim, Phys. Rev. C **19**, 1344 (1979).
¹⁷C. J. Gross, P. D. Cottle, D. M. Headly, U. J. Hüttmeier, E. F. Moore, and S. L. Tabor, Phys. Rev. C **36**, 2127 (1987).
¹⁸J. Adam, M. Honusek, A. Spalek, D. N. Doynikov, A. D. Efimov, M. F. Kudojarov, I. Kh. Lemberg, A. A. Pasternak, O. K. Vorov, and U. Y. Zhovliev, Z. Phys. A **332**, 143 (1989).
¹⁹R. Bengtsson, S. Frauendorf, and F. -R. May, At. Data Nucl. Data Tables **35**, 15 (1986).
²⁰H. P. Hellmeister, U. Kaup, J. Keinonen, K. P. Lieb, R. Rascher, R. Ballini, J. Delauney, and H. Dumont, Phys. Lett. **85B**, 34 (1979).
²¹B. Wörmann, K. P. Lieb, R. Diller, L. Lühmann, J. Keinonen, L. Cleemann, and J. Eberth, Nucl. Phys. A **431**, 170 (1984).
²²W. Nazarewicz, J. Dudek, R. Bengtsson, T. Bengtsson, and I. Ragnarsson, Nucl. Phys. A **435**, 397 (1985).
²³D. F. Winchell, M. S. Kaplan, J. X. Saladin, H. Takai, J. J. Kolata, and J. Dudek, Phys. Rev. C **40**, 2672 (1989).
²⁴W. Nazarewicz, private communication.
²⁵U. J. Hüttmeier, C. J. Gross, D. M. Headly, E. F. Moore, S. L. Tabor, T. M. Cormier, P. M. Swertka, and W. Nazarewicz, Phys. Rev. C **37**, 118 (1988).